

## Supplementary Information

### **Li<sub>1.6</sub>AlCl<sub>3.4</sub>S<sub>0.6</sub>: A Low-Cost and High-Performance Solid Electrolyte for Solid-State Batteries**

*Tej P. Poudel, <sup>†</sup> Ifeoluwa P. Oyekunle, <sup>†</sup> Michael J. Deck, Yudan Chen, Dewen Hou, Pawan K. Ojha, Bright O. Ogbolu, Chen Huang, Hui Xiong, Yan-Yan Hu\**

Dr. T.P. Poudel, Dr. Y.-Y. Hu

Materials Science and Engineering Program  
The Graduate School, Florida State University  
2005 Levy Ave., Tallahassee, FL 32310, USA

Dr. T.P. Poudel, I.P. Oyekunle, Dr. M.J. Deck, Y. Chen, P.K. Ojha, Bright Ogbolu, Dr. Y.-Y. Hu  
Department of Chemistry and Biochemistry  
Florida State University  
95 Chieftan Way, Tallahassee, FL 32306, USA

Dr. D. Hou

Center for Nanoscale Materials Argonne National Laboratory  
9700 S Cass Ave, Lemont, IL 60439, USA

Dr. Hui Xiong

Micron School of Materials Science and Engineering  
Boise State University, Boise, ID, 83725, USA

Dr. T.P. Poudel, I.P. Oyekunle, Dr. M.J. Deck, Y. Chen, P.K. Ojha, Bright Ogbolu Dr. Y.-Y. Hu  
Center of Interdisciplinary Magnetic Resonance  
National High Magnetic Field Laboratory  
1800 East Paul Dirac Drive, Tallahassee, FL 32310, USA

Orcid:

Tej P. Poudel: 0000-0003-4787-5739

Ifeoluwa P. Oyekunle: 0000-0001-7623-4493

Michael J. Deck: 0000-0001-6439-8634

Yudan Chen: 0000-0003-1495-4289

Dewen Hou: 0009-0006-8779-6559

Pawan K. Ojha: 0000-0003-1503-0029

Bright Ogbolu: 0000-0003-1048-0506

Chen Huang: 0000-0003-2934-8118

Hui Xiong: 0000-0003-3126-1476

Yan-Yan Hu: 0000-0003-0677-5897

\*Corresponding author: [yhu@fsu.edu](mailto:yhu@fsu.edu)

† Authors contributed equally

**Keywords:** solid electrolytes; chalcohalide; local disorder; solid-state NMR; energy storage; batteries

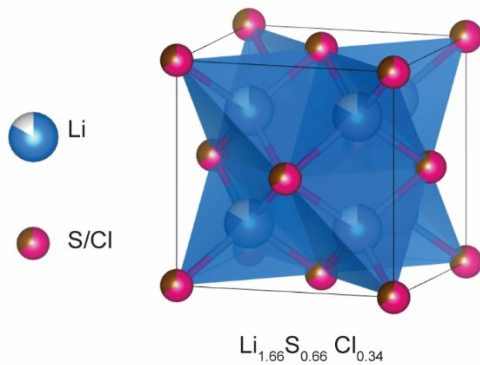


**Figure S1.** The structure of  $\text{Li}_{1.66}\text{S}_{0.66}\text{Cl}_{0.34}$ , a minor component observed from high-resolution X-ray diffraction and  ${}^6\text{Li}$  MAS NMR in the  $\text{Li}_{1.6}\text{AlCl}_{3.4}\text{S}_{0.6}$  sample.

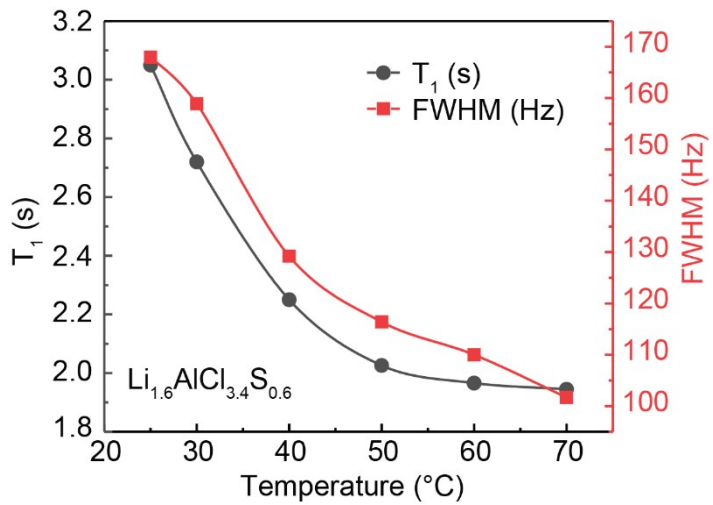


**Figure S2.** Variable-temperature  $^7\text{Li}$   $T_1$  NMR relaxation time measurements for  $\text{Li}_{1.6}\text{AlCl}_{3.4}\text{S}_{0.6}$  to probe  $\text{Li}^+$  dynamics.

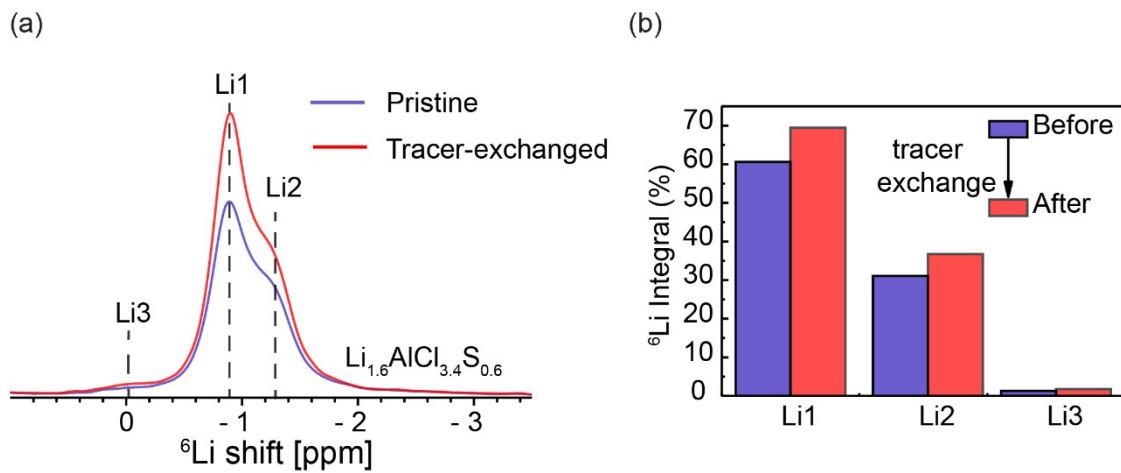


**Figure S3.**  $^6\text{Li} \rightarrow ^7\text{Li}$  tracer-exchange NMR confirms the active role of the Li sites in  $\text{Li}_{1.6}\text{AlCl}_{3.4}\text{S}_{0.6}$

(a) The comparison of the  $^6\text{Li}$  MAS NMR spectra of pristine and tracer-exchanged (driven via electrochemical cycling)  $\text{Li}_{1.6}\text{AlCl}_{3.4}\text{S}_{0.6}$ ; and (b) quantification of Li sites in  $\text{Li}_{1.6}\text{AlCl}_{3.4}\text{S}_{0.6}$  before and after  $^6\text{Li} \rightarrow ^7\text{Li}$  tracer-exchange.

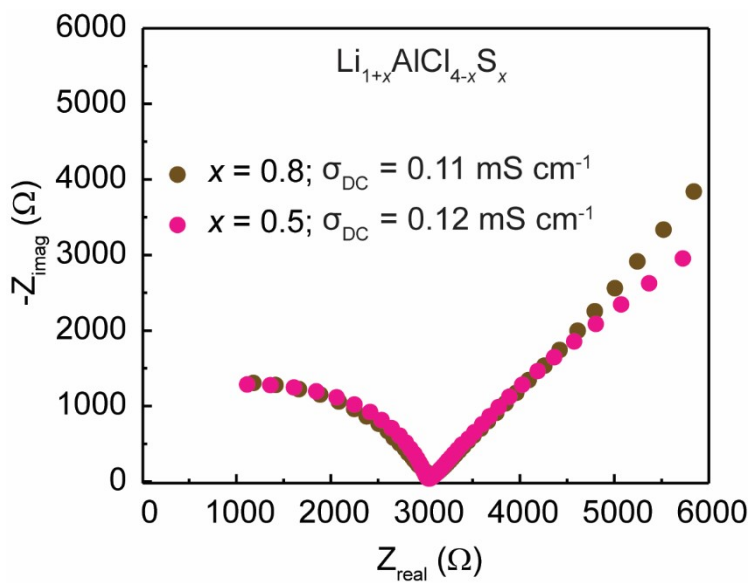


**Figure S4.** Nyquist plots of  $\text{Li}_{1.5}\text{AlCl}_{3.5}\text{S}_{0.5}$  and  $\text{Li}_{1.8}\text{AlCl}_{3.2}\text{S}_{0.8}$

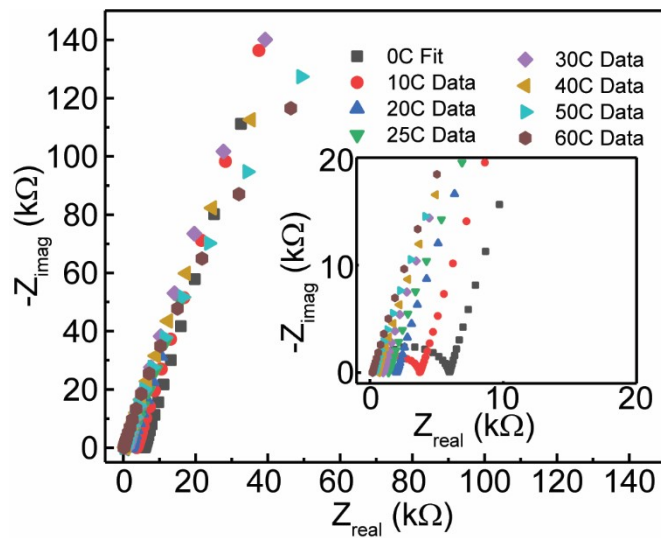


**Figure S5.** Representative Nyquist plots from variable-temperature electrochemical impedance spectroscopy of  $\text{Li}_{1.6}\text{AlCl}_{3.4}\text{S}_{0.6}$ .

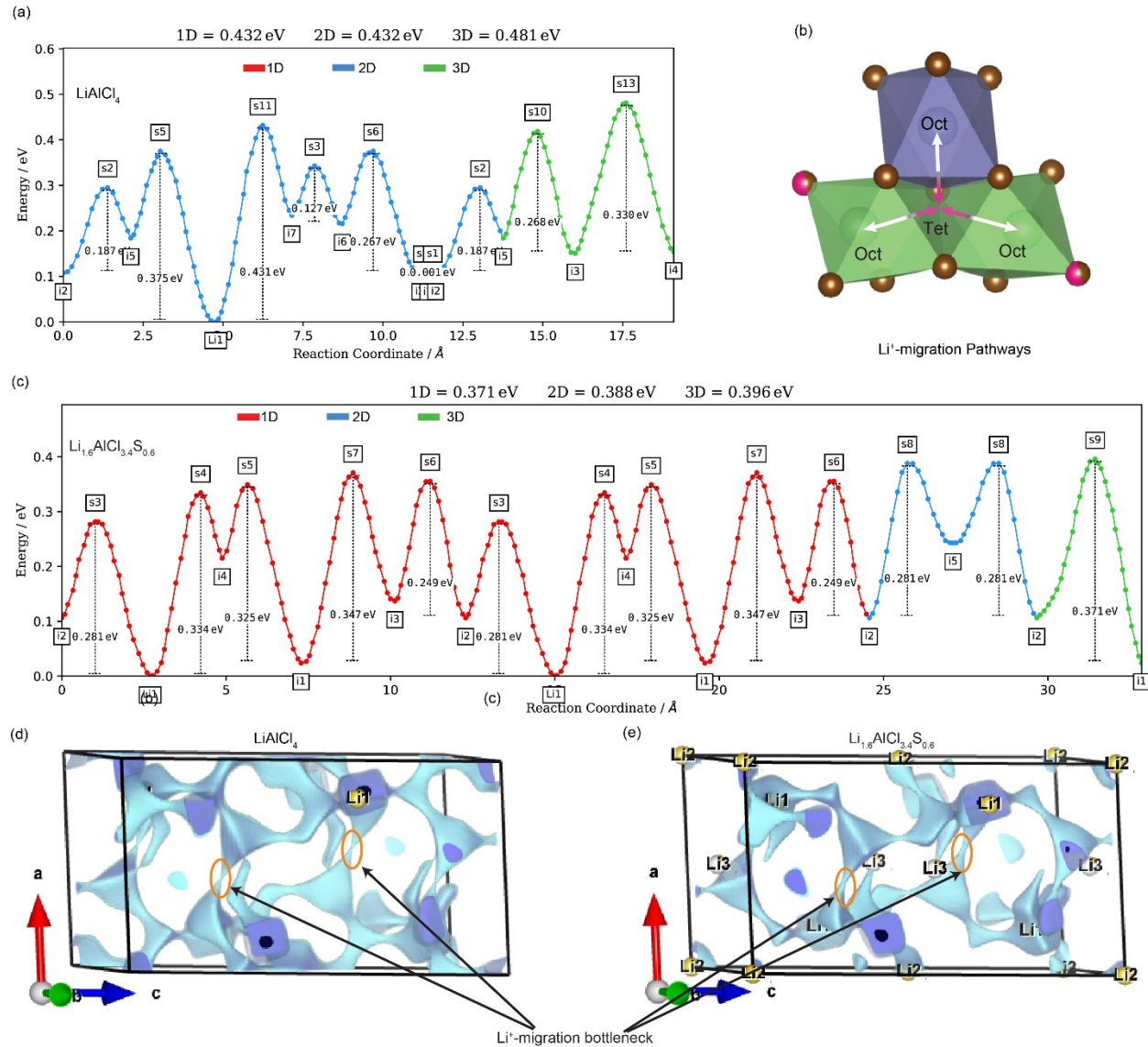


**Figure S6.** BVSE calculation and its energy landscape of (a) LiAlCl<sub>4</sub> (c) Li<sub>1.6</sub>AlCl<sub>3.4</sub>S<sub>0.6</sub>. (b) Possible Li-ion migration pathways in Li<sub>1.6</sub>AlCl<sub>3.4</sub>S<sub>0.6</sub>. The Li-isosurfaces of (d) LiAlCl<sub>4</sub> (e) Li<sub>1.6</sub>AlCl<sub>3.4</sub>S<sub>0.6</sub> structures.

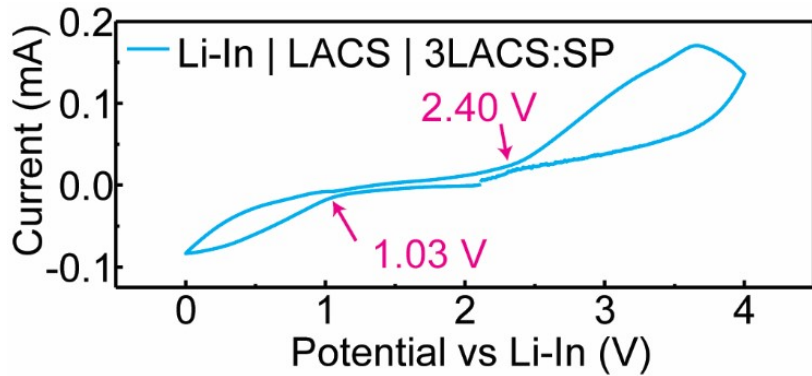


**Figure S7.** Cyclic voltammogram of  $\text{Li}_{1.6}\text{AlCl}_{3.4}\text{S}_{0.6}$  using carbon black (Super P) as the electronic conductive medium in  $3\text{Li}_{1.6}\text{AlCl}_{3.4}\text{S}_{0.6}:\text{SP}$ . An electrochemical stability window of 1.03 V to 2.40 V is obtained for  $\text{Li}_{1.6}\text{AlCl}_{3.4}\text{S}_{0.6}$ .

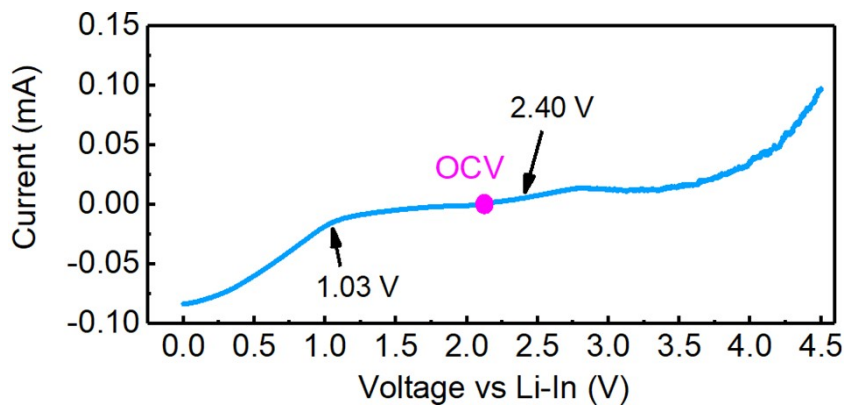


**Figure S8.** Linear Sweep voltammogram of  $\text{Li}_{1.6}\text{AlCl}_{3.4}\text{S}_{0.6}$  using carbon black (Super P) as the electronic conductive medium in  $3\text{Li}_{1.6}\text{AlCl}_{3.4}\text{S}_{0.6}:\text{SP}$ . An electrochemical stability window of 1.03 V to 2.40 V is obtained for  $\text{Li}_{1.6}\text{AlCl}_{3.4}\text{S}_{0.6}$ .

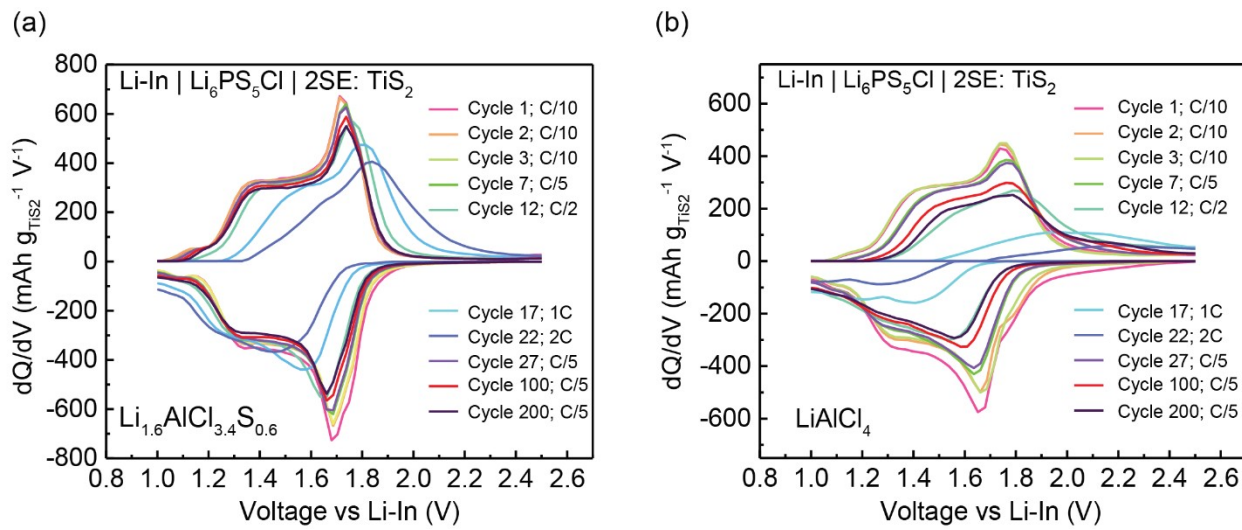


**Figure S9.** The differential capacity plots of Li-In | LPSCl | 2SE:TiS<sub>2</sub> cells using (a) Li<sub>1.6</sub>AlCl<sub>3.4</sub>S<sub>0.6</sub> and (b) LiAlCl<sub>4</sub> as the solid electrolyte (SE).

**Table S1.** Rietveld-refinement results of high-resolution X-ray diffraction data at room temperature for the mechanochemically synthesized LiAlCl<sub>4</sub>.

LiAlCl<sub>4</sub> – Ball milled for 20 h.

Composition: LiAlCl<sub>4</sub>

Lattice parameter:  $a = 7.0035(7)$ ,  $b = 6.5088(6)$ ,  $c = 13.0008(8)$ ,  $\alpha = \gamma = 90.000$ ,  $\beta = 93.34(7)$ ,

Unit-cell volume =  $591.62(8)$  Å<sup>3</sup>

Density of LiAlCl<sub>4</sub> = 1.973 g/cm<sup>3</sup>

$R_{wp} = 5.482\%$ , Space group P21/c, Impurity phases: 2.8 wt% of LiCl

Name	Atom	Wycoff position	Atomic coordinates			Occupancy	$U_{iso}$
			x	y	z		
Li1	Li	4e	0.176(3)	1.009(4)	0.380(2)	1	0.038(6)
Al1	Al	4e	0.7098(8)	0.329(1)	0.9006(5)	1	0.039(2)
Cl1	Cl	4e	0.6944(8)	0.1834(8)	0.0459(5)	1	0.045(2)
Cl2	Cl	4e	0.8085(8)	0.6225(8)	0.9265(5)	1	0.036(2)
Cl3	Cl	4e	0.9232(8)	0.1819(9)	0.8136(5)	1	0.038(2)
Cl4	Cl	4e	0.4469(8)	0.3062(8)	0.8127(5)	1	0.035(2)

**Table S2.** Rietveld-refinement results of the high-resolution X-ray diffraction data for the mechanochemically synthesized  $\text{Li}_2\text{AlCl}_3\text{S}$ .

Refined composition :  $\text{Li}_{1.6}\text{AlCl}_{3.4}\text{S}_{0.6}$

Lattice parameter:  $a = 7.0207(8)$ ,  $b = 6.5206(8)$ ,  $c = 13.004(2)$ ,  $a = g = 90.0000$ ,  $b = 93.43(1)$ ,

Unit-cell volume =  $594.26(8) \text{ \AA}^3$ ;

Density of  $\text{Li}_{1.6}\text{AlCl}_{3.4}\text{S}_{0.6} = 1.984 \text{ g cm}^{-3}$

$R_{wp} = 2.85 \%$ , Space group  $P2_1/c$

Impurity phases: 14 wt% of  $\text{Li}_2\text{S}$  and 10 wt% of  $\text{Li}_{1.66}\text{S}_{0.66}\text{Cl}_{0.34}$

Name	Atom	Wycoff	Atomic coordinates			Occupancy	$U_{iso}$
			position	x	y		
Li1	Li	4e	0.198(1)	0.035(1)	0.349(6)	1	0.14(4)
Li2	Li	2a	0	0	0	1(4)	0.08(2)
Li3	Li	2a	0.5	0	0.5	0.17(3)	0.59(7)
Al2	Al	4e	0.728(2)	0.335(2)	0.898(1)	1	0.057(3)
Cl1	Cl	4e	0.685(2)	0.200(2)	0.043(1)	1	0.025(5)
Cl2	Cl	4e	0.955(2)	0.164(2)	0.809(1)	1	0.032(3)
Cl3	Cl	4e	0.812(2)	0.622(1)	0.925(1)	1	0.032(3)
Cl4	Cl	4e	0.464(2)	0.296(2)	0.806(1)	0.519(6)	0.065(6)
S4	S	4e	0.464(2)	0.296(2)	0.806(1)	0.481(6)	0.065(6)

**Table S3.** Rietveld-refinement results of the  $\text{Li}_{1.66}\text{S}_{0.66}\text{Cl}_{0.34}$ -phase present in  $\text{Li}_2\text{AlCl}_3\text{S}$ .

Refined composition:  $\text{Li}_{1.66}\text{S}_{0.66}\text{Cl}_{0.34}$

Lattice parameter:  $a = 5.7138(7)$ ,  $a = b = g = 90.0000$ ,

Unit-cell volume =  $186.64(5) \text{ \AA}^3$ ;

Density of  $\text{Li}_{1.66}\text{S}_{0.66}\text{Cl}_{0.34} = 1.592 \text{ g/cm}^3$

Space group  $Fm-3m$

Name	Atom	Wycoff	Atomic coordinates			Occupancy	$U_{iso}$
			position	x	y		
Li	Li	8c	0.25	0.25	0.25	0.83(1)	0.015(5)

S	S	4a	0	0	0	0.66(1)	0.012(1)
Cl	Cl	4a	0	0	0	0.34(2)	0.012(2)

**Table S4.** Li (%) distribution in various components in  $\text{LiAlCl}_4$  and  $\text{Li}_{1.6}\text{AlCl}_{3.4}\text{S}_{0.6}$  from  ${}^6\text{Li}$  NMR analysis.

Sample	${}^6\text{Li}$ (%)					
	Li1	Li2	Li3	$\text{Li}_2\text{S}$	LiCl	$\text{Li}_{1.66}\text{S}_{0.66}\text{Cl}_{0.34}$
$\text{LiAlCl}_4$	92.5	-	-	-	7.5	-
$\text{Li}_{1.6}\text{AlCl}_{3.4}\text{S}_{0.6}$	60.6	31.1	1.3	3.1	-	3.9